Wave separation analysis to assess cardiovascular alterations induced by sepsis

Diletta Guberti, Manuela Ferrario, Shengchen Liu, Stephan M. Jakob, and Marta Carrara*

***Abstract*— *Objective:* Sepsis induces a severe decompensation of arterial and cardiac functional properties, leading to important modifications of arterial blood pressure (ABP) waveform, not resolved by recommended therapy, as shown by previous works. The aim of this study is to quantify the changes in ABP waveform morphology and wave reflections during a long-term swine experiment of polymicrobial sepsis and resuscitation, to deepen the understanding of the cardiovascular response to standard resuscitation therapy. *Methods*: We analyzed 14 pigs: polymicrobial sepsis was induced in 9 pigs followed by standard resuscitation and 5 pigs were treated as sham controls. Septic animals were studied at baseline (T1), after sepsis development (T2), and after 24h (T3) and 48h (T4) of therapy administration, and sham controls at the same time points. ABP and arterial blood flow were measured in the left and right carotid artery, respectively. Pulse wave analysis and wave separation techniques were used to estimate arterial input impedance, carotid characteristic impedance, forward and backward waves, indices of wave reflections such as reflection magnitude and reflection index, and augmentation index. *Results:* Sepsis led to an acute alteration of ABP waveform passing from type A to type B or C; consistently, the reflection phenomena were significantly reduced. The resuscitation was successful in reaching targeted hemodynamic stability, but it failed in restoring a physiological blood propagation and reflection. *Conclusion:* Septic pigs persistently showed altered reflected waves even after 48 hours of successful therapy according to guidelines, suggesting a persistent hidden cardiovascular disorder. *Significance:* The proposed indices may be useful to unravel the complex cardiovascular response to therapy administration in septic patients and could potentially be used for risk stratification of patient deterioration. Whether alterations of blood propagation and reflection contribute to persisting organ dysfunction after hemodynamic stabilization should be further investigated.**

***Index Terms*— arterial impedance; hemodynamic monitoring; pulse wave analysis; sepsis; wave reflections.**

I. Introduction

SEPSIS is a widespread condition associated with unacceptably high mortality and long-term morbidity for many of those who survive [1]. Its occurrence ranges from 13.9% to 39.3% of ICU admissions worldwide [2], and it is one of the major causes of mortality in the ICU, accounting for almost 20% of all global deaths [3]. Surviving patients often have long-term deficits, including cognitive impairments and cardiovascular diseases [4]. It is estimated that nearly a quarter of sepsis survivors will be readmitted to hospital within 30 days of discharge [5], and their mortality rate within 5 years may be as high as 75% [6].

Septic patients are typically resuscitated based on global hemodynamic targets, such as mean arterial pressure and oxygenation [7], that convey system-wide information only, without any pathophysiological clue about the biomechanical and functional properties of the cardiovascular system, such as ventricular afterload, vascular tone, and wave reflections, which are highly dependent also on the pulsatile component of blood pressure [8]–[10].

Previous studies of our group on several animal populations undergoing different resuscitation protocols highlighted how the arterial blood pressure (ABP) waveform and the cardiovascular function were profoundly altered by sepsis progression. In addition, the standard therapy administration wasn't able to restore the physiological condition neither in septic shock pigs on a short time window of ~5/6 hours nor in septic pigs over a longer observational time interval of 72 hours, although in both cases the resuscitation was considered successful on the basis of standard parameters [11], [12]. In particular, the computed indices pointed out a stiffening of the large arteries (e.g., aorta or carotid artery) and a loss of peripheral resistance [12]–[15], a condition which led to peripheral vascular decoupling, i.e. an inversion of the physiological amplification of pulse pressure (PP) from central to peripheral sites [11], [16]. All these observations support the hypothesis of a persistent hidden cardiovascular disorder in subjects evaluated effectively resuscitated. Moreover, the ABP waveform was substantially far from a physiological morphology after resuscitation, hinting that blood flow transmission and reflection are also impaired [11], [12], [15].

The technological advances in terms of monitoring systems and data processing could help in defining and measuring novel hemodynamic therapy targets. In this context, the pulse wave analysis (PWA) could play an important role. PWA and wave separation techniques have been proposed originally to monitor patients with chronic diseases, such as those affected by hypertension or elderly

D. G., M. F., and M.C. are with Department of Electronics, Information and Bioengineering, Politecnico di Milano, Milan, Italy. S. L. and S. J. are with University of Bern, Bern, Switzerland (correspondence e-mail: marta.carrara@polimi.it).

patients. Here, the vascular properties are structurally altered, and therefore generate important alterations of reflection phenomena and pulse wave morphology, and, thereby, modifications of the cardiovascular interactions [17]–[20]. However, critical illness induces *acute* functional alterations of cardiac and arterial properties, at the same time the rapid therapeutic interventions typically prescribed in the intensive care unit (ICU), e.g., vasopressor administration, organ support, fluids infusion, may further stress the cardiovascular system, as our preliminary results have shown. For example, large artery stiffness, peripheral resistance, microvascular properties, cardiac contractility, and heart rate, which sepsis and resuscitation greatly affect, all influence the pattern of pressure/flow waves measured in blood vessels [10]; therefore, PWA and wave separation techniques may represent a powerful tool to extract additional information to evaluate the cardiovascular system status during sepsis and the response to the administered therapy. However, the use of these techniques in acute critically ill patients is limited.

The primary objective of this study is to investigate the changes in ABP waveform morphology and wave reflections during a long-term swine experiment of polymicrobial sepsis and resuscitation. Firstly, we were interested in testing the feasibility of using PWA and wave separation techniques in a complex and highly nonstationary setting; secondly, we wanted to verify if these techniques were able to capture the hemodynamic alterations in septic subjects; finally, we aimed at deepening the understanding of the cardiovascular response to standard resuscitation therapy in septic shock.

Hemodynamic signals, such as invasive ABP, are typically continuously recorded in ICU patients, and this explorative research may help in identifying some potential mechanisms at the basis of the well-known cardiovascular complications affecting surviving septic patients, such as vascular senescence. In addition, the results could potentially also be used for risk stratification of patient deterioration [21], [22].

II. Methods

A. Experimental protocol and data acquisition

This study was carried out in collaboration with the Inselspital University Hospital of Bern, Switzerland. The animal protocol was performed in accordance with the EU Directive 2010/63/EU for animal experiments and the ARRIVE guidelines for animal research, and with the approval of the Animal Care Committee of the Canton of Bern (BE103/16). Previous works have been already published on the same experiment [12], [23], [24].

Twenty domestic pigs (weight: 39.8 ± 2.7 kg; male/female: 1:1) were used for the experiment. Details about surgical preparation and instrumentation are reported in previous works [25] and in the supplementary materials. After instrumentation, one-hour stabilization was allowed, followed by baseline blood sampling (time point T1). Then, the pigs were randomized to fecal peritonitis (SS n = 10)/sham (SH n = 10). Sepsis was induced by peritoneal instillation of 2 g/kg of autologous feces dissolved in 250 mL warmed glucose 5% solution. After 8h of observation without resuscitation, another set of blood samples were collected (T2), referring to the septic condition. Then, protocol-based resuscitation was started and continued for three days (resuscitation period, RP), including fluid infusion (e.g., ringer lactate), vasopressor support (e.g., noradrenaline), electrolyte maintenance, antibiotic therapy, and reduction of body temperature, if needed. Details about resuscitation maneuvers can be found in the supplementary material. Further blood samplings were done at RP + 24 h (T3), RP + 48 h (T4) and at the end of the experiment, approximately 72 hours after start of resuscitation (T5). At the end of the experiment the animals were deeply sedated and euthanized by bolus infusion of 40 mmol of potassium chloride.

During animals' instrumentation, an open surgical approach with visualization of the carotid arteries was followed with the pig in supine position. A midline neck incision was performed to allow placement of an arterial catheter (5F, Cordis AVANTI, Fremont, CA, USA) in the left carotid artery toward the heart (against the direction of cerebral blood flow) for continuous registration of carotid ABP, and an ultrasound Doppler flow probe (Transonic Systems Inc., Ithaca, NY, USA) around the right carotid artery to continuously acquire arterial blood flow signals. A schematic picture of the carotid sensors' placement is provided in the Supplementary material. The signals were recorded at 100 Hz by a data acquisition system (Soleasy™; National Instruments Corp., Austin, Tx, USA). The time points used for blood sample analyses were considered as reference to identify and select portions of signals (5-10 minutes) for successive analyses.

The sample size in the original study [24] was n=20. Due to technical reasons the blood flow signal was noisy and of poor quality in some pigs at certain time points, therefore such signals were excluded from the analyses. The final dataset used in this work consists of 14 pigs: 5 for the sham group and 9 for the septic group.

B. Pulse wave propagation and reflection: theoretical background

The measured arterial pulse wave is typically composed of a forward (or incident) and a backward (or reflected) wave, that is generated whenever the forward travelling wave encounters impedance changes resulting from geometrical factors (branching, diameter tapering) and tissue property variations (stiffness and stiffness gradient) [26]. In physiological conditions the amplitude of arterial pulse is increasing from central to peripheral sites, named PP amplification, due to wave reflections phenomena [10]. Moreover, wave reflections physiologically act as a protective mechanism to avoid excessive pulsatility into the microcirculation: indeed, partial wave reflection returns a portion of the pulsatile energy content of the waveform to the central aorta where it is dissipated by viscous damping [19].

The magnitude and timing of reflected waves heavily affect the morphology of the ABP waveform measured

centrally, and, indirectly, the cardiac workload [10]. In fact, if the reflected wave arrives earlier during systole (type A waveform) it contributes to the rise of systolic pressure and the increase of cardiac afterload; otherwise, if the reflected wave arrives later after the systolic peak (type C waveform), it contributes more to the myocardial perfusion gradient in the coronary arteries (Fig. 1). Type B (not here illustrated) corresponds instead to the case where inflection point (IP), i.e. the time of arrival of reflected waves, coincides with the ABP peak.

Generally, the opposition of the vascular system to the pulsatile flow ejected by the heart can be described in terms of input impedance Z_{in}, which is intrinsically a frequency domain quantity, and it is defined as the ratio of pressure harmonics to flow harmonics at the entrance of the system. It depends on the dimensions and viscoelasticity properties of the arteries, on the physical properties of blood, and on the reflected wave [10], [27]. If the arterial tree were a reflectionless system, the pressure and flow waves would have similar shape and their relationship would be estimated by the characteristic impedance *Zc* of the vessel. Since wave reflections carry information about the distal vasculature, their exclusion makes *Zc* a local vessel parameter, independent of heart rate as well as properties of the downstream vascular beds. *Zc* depends on vessel size, wall stiffness (compliance) and blood properties, it can be seen as the result of the accelerating blood mass taking place during the ejection phase into the compliant artery; therefore, the stiffer the vessel and the smaller its diameter, the higher the value of *Zc* [28].

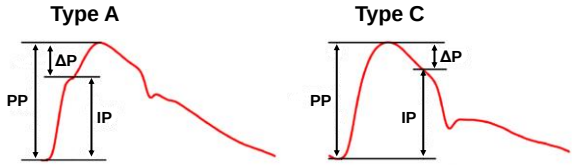

Fig. 1. Example of type A waveform (left panel) and type C waveform (right panel). Δ*P*: augmented pressure [mmHg]; PP: pulse pressure [mmHg]; IP: inflection point [mmHg], which coincides with the arrival time of reflected wave.

C. Arterial pulse wave analysis

The ABP and arterial blood flow (ABF) waveforms were first filtered by a moving average low-pass filter with different order to remove the noisy high-frequency oscillations eventually superimposed to the signals. The order of the filter was ranging from 2 to 5. Hence, ABP and ABF beats onsets were identified using the algorithm proposed by Zong and colleagues [29]. Beat-to-beat indices were then computed from ABP as follows: systolic arterial pressure (SAP), corresponding to the maximum value within each beat, diastolic arterial pressure (DAP), corresponding to the minimum value within the beat, mean arterial pressure (MAP), obtained by averaging all the values within the beat, pulse pressure (PP), defined as the difference between SAP and DAP, heart period (HP), computed as the time difference between consecutive onsets and representing a surrogate for RR-intervals. The inflection point (IP) was identified using the algorithm described in [30] which is based on signal derivative of different orders. Augmented pressure (Δ*P*) was computed as the difference between SAP and IP for type A pulse or as the difference between IP and SAP for type B/C pulse (Fig. 1). Augmentation index (AIx) was computed as the percentage ratio between Δ*P* and PP:

$$AIx = \frac{\Delta P}{PP} * 100 \quad (1)$$

Heart rate (HR) was computed as $HR = 60/HP$ $[bpm]$. The beat-to-beat series of mean ABF was computed by averaging all the values of ABF within each beat.

All the beat-to-beat time series were then averaged to obtain one value for each pig at each time point. These values were then used for successive statistical analyses.

D. Wave separation analysis and estimation of the characteristic impedance Zc

Vascular impedance was estimated on a beat template obtained by averaging three consecutive beats manually selected at each time point. The ABF and ABP beat templates were aligned so that the onset of blood pressure coincides with the onset of the blood flow. The alignment was carefully checked by visual inspection, we verified that the morphological features of blood and flow were consistent, e.g., if beat of type A, the flow peak should occur in correspondence of pressure inflection point, whereas if beat of type B, the flow peak and the pressure peak are typically simultaneous; in addition, the occurrence of the dicrotic notch should coincide with the end of flow. Moreover, the times of all recording devices were synchronized before each experiment, and the end of the recordings - when death of the animals occurred – were compared to make sure that no time shift had evolved during the experiment between devices.

Characteristic impedance (*Zc*) was determined by means of both time and frequency domain approaches. Time domain methods included: *i*) the *up-slope method*, i.e. Zc is estimated from the slope of pressure-flow loop during early ejection phase (95% of maximum flow) [31], [32]; *ii*) the *maximum derivative method*, i.e. Zc is estimated by the ratio max(ABP')/max(ABF'), where ABP' and ABF' are the first order derivatives of ABP and ABF, respectively [31].

Assuming that the cardiovascular system is linear and over few beats the pulse waves can be considered of the same duration T_0, ABP and ABF can be decomposed in their harmonics by computing the Fourier Series coefficients over a single or multiple heartbeats [31], *Zin* can be then expressed in terms of modulus and phase:

$$|Zin|_k = \frac{ABP_k}{ABF_k} \quad (2)$$

$$\xi_k = \Phi_k - \Psi_k \quad (3)$$

where $|Zin|_k$ and ξ_k are the modulus and phase of *Zin* spectrum, respectively, *k* represents the k^{th} harmonic multiple of the fundamental frequency $f_0=1/T_0$, ABP_k and ABF_k are the pressure and flow modulus of the k^{th} harmonic, and Φ_k and Ψ_k are the pressure and flow phase of the k^{th} harmonic,

respectively. *Zc* can be obtained by averaging *Zin* modulus in a range of high frequency harmonics from the i^{th} to the j^{th}:

$$Z_c = \frac{1}{j-i+1}\sum_{k=i}^{j}|Y_k| \quad where\ Y_k = \frac{ABP_k}{ABF_k} \tag{4}$$

In this work we adopted *i*=2 and *j*=8. However, in septic shock condition, we observed the typical "bell-shape" type B waveform, which is a much simpler waveform that can be described with fewer coefficients, so we used *i*=2 and *j*=5 in this case.

Once Zc have been estimated, the forward P_f and backward P_b waves, can be computed as follows [28]:

$$P_f = \frac{ABP+Z_c*ABF}{2} \tag{5}$$

$$P_b = \frac{ABP-Z_c*ABF}{2} \tag{6}$$

The amplitude of P_b and P_f was estimated as the difference between the maximum and the minimum value. The wave reflection transit time (Tr) was computed as the time difference between the onset of the beat and the time of arrival of the backward wave.

E. Wave reflection indices

Several indices have been proposed to assess the amount of wave reflection and how it changes during the experiment [10]. *Reflection magnitude (RM)* generally quantifies the amount of reflection, and it has been computed as the ratio between the amplitude of the backward to the forward wave:

$$RM = \frac{|P_b|}{|P_f|} \tag{7}$$

Reflection index (RI) indicates the amount of reflection occurring with respect to the total wave, and it is defined as:

$$RI = \frac{|P_b|}{|P_f|+|P_b|} \tag{8}$$

The *first harmonic of the Zin normalized by Zc* has been proposed in the past as an index of the global amount of reflections in the system [33], [34], and also recently it has been shown to be strictly related to the reflection coefficient both in type A and type C beats [26]. It is computed as the ratio between the first harmonic of Zin and Zc:

$$|Zin|_1 normalized = \frac{|Zin|_1}{Z_c} \tag{9}$$

F. Waveform complexity

We adopted the *Harmonic Distortion (HD)* index to investigate the complexity of the arterial pressure waveform. HD is computed as

$$HD = \frac{\sum_{k=2}^{6}|ABP_k|^2}{|ABP_1|^2} \tag{10}$$

Where ABP_1 is the fundamental harmonic component. HD can be seen as the ratio of the energy above the fundamental frequency over the energy at the fundamental frequency of the waveform [35], therefore it may be used to quantify the "complexity" of the pulse wave, i.e., a ABP waveform consisting of fewer reflected waves should be a "simpler" waveform and HD index value should be lower according to its mathematical meaning. The ideal case for a signal composed by only a sinusoid, i.e. by only the harmonic *k*=1, HD would be equal to 0. Although HD has been recently proposed as a possible surrogate index of arterial stiffness [35], [36], in this work we aimed only at testing whether HD is related to the amount of reflected waves.

G. Laboratory variables

The following laboratory variables were measured at each time point: band neutrophils percentage (N%, [%]), which is a measure of infection or inflammation, hemoglobin (Hb, [g/L]), hematocrit (Htc, [L/L]), lactate [mmol/L], mixed venous oxygen saturation (SvO2, [%]).

H. Statistical analyses

Wilcoxon rank-sum test was adopted to verify significant differences in the indices between the two groups at each time point. Friedman test was adopted to find differences within each group among time points across multiple tests attempts. In case of significant Friedman test p-value, the Wilcoxon signed-rank test was used to assess significant changes among pairs of time points within each group of animals. For the post-hoc multiple comparisons we adopted the Tukey's honestly significant difference correction for p-value significance. Significance was considered with a p-value < 0.05.

The different estimates of *Zc* have been compared by means of Bland-Altman plots and correlation analysis.

III. Results

Table I shows the number of pigs analyzed at each time point. Time point T5 was excluded from the analyses because the quality of ABF signal was very poor for most of the pigs. An example of a low-quality ABF is illustrated in the supplementary material.

TABLE I
NUMBER OF PIGS AVAILABLE FOR THE ANALYSES AT EACH TIME POINT

	T1	T2	T3	T4	T5
SS	9/9	9/9	9/9	8/9	/
SH	5/5	5/5	4/5	3/5	/

SS: septic pigs (9 in total), SH: sham pigs (5 in total), T1: baseline, T2: after sepsis development, T3: after 24h of resuscitation, T4: after 48h of resuscitation, T5: after ~72h of resuscitation.

A. Hemodynamic variables and laboratory parameters

Table II reports the values of laboratory and hemodynamic variables at all time points for SS and SH pigs. The septic state (T2) of SS pigs is confirmed by a marked increase in band neutrophil amount (N%) and by the inflammatory response which resulted in an increased endothelial permeability and capillary leakage as the significant increase in Htc and Hb values corroborate; the septic associated hypotension and hypovolemia were confirmed by the

significant decrease of blood pressure and blood flow values, and tissue hypoperfusion was further suggested by the increase in lactate concentration and the decrease in mixed venous oxygen saturation. Moreover, the hypotensive state together with the systemic inflammation triggered tachycardia in SS pigs, resulting in a significantly higher HR compared to SH group at T2.

The main target of hemodynamic resuscitation, according to international guidelines, is to restore a MAP $\geq$ 65 mmHg by means of fluids and vasopressors therapy and to maintain a sufficient organ oxygen supply [7]. In our protocol, the resuscitation strategy was effective in restoring and keeping MAP in the target range and to significantly increase SvO_2 which was maintained above 60% in almost all animals. However, the tachycardic response was not resolved at T3 and T4, remaining significantly higher in SS pigs compared to SH pigs.

B. Pulse wave indices

Sepsis induced a profound change in ABP waveform in all SS pigs: a typical type A pulse was observed at baseline (T1) and a type B or C pulse at T2 (Fig. 2). Fig. 3 shows the values distribution of PP, ΔP, and AIx at each time point. Septic pigs were characterized by a significant decrease of all indices at T2 induced by the septic condition; the values of AIx became negative in almost all SS pigs, consistently with the fact that the ABP waveform passes from type A to type B or C. During resuscitation (T3, T4) the values were gradually restored to be similar to those at baseline and in SH pigs, although with a pronounced inter-subject variability.

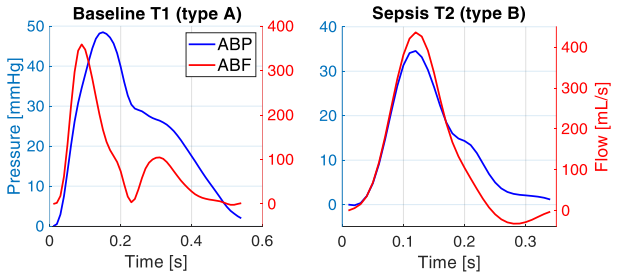

Fig. 2. Example of type A waveform (left panel) typically found at baseline, and type B waveform (right panel), typically observed after sepsis development.

TABLE II
MEDIAN (25TH-75TH PERCENTILES) VALUES OF LABORATORY AND HEMODYNAMIC VARIABLES AT EACH TIME POINT FOR THE TWO GROUPS

		T1	T2	T3	T4
LAB VARIABLES					
N%	SS	5.5 (0.8,14.0) [n=8]	48.0 (38.6,58.6) °	33.5 (26.1,48.8) °	14.0 (11.5,20.0) #
	SH	4.0 (3.4,11.9)	0.0 (0.0,0.5) *°	0.0 (0.0,0.13) *°	0.0 (0.0,1.0) *
Hb	SS	101 (91,102)	132 (119,141)	100 (94,106)	83 (76,89) #
	SH	98 (90,102)	95 (84,96) *	72 (65,80) *°	76 (55,77) *°#
Htc	SS	0.29 (0.28,0.31) [n=8]	0.38 (0.36,0.41)	0.29 (0.29,0.31)	0.25 (0.23,0.26) #
	SH	0.29 (0.27,0.31)	0.28 (0.25,0.29) *	0.22 (0.20,0.24) *°	0.22 (0.17,0.23) *°#
Lact	SS	0.6 (0.5,0.7)	0.8 (0.7,1.2)	0.8 (0.6,1.0)	0.7 (0.5,0.9) #
	SH	0.8 (0.5,0.9)	0.5 (0.4,0.5) *	0.3 (0.2,0.3) *	0.2 (0.2,0.3) *°
SvO2	SS	57.3 (53.0,62.8)	46.0 (42.0,56.3)	63.5 (61.4,67.9) ##	66.6 (62.6,67.2) ##
	SH	57.0 (54.9,62.5)	53.0 (50.3,55.4)	55.8 (47.5,56.3)	55.1 (51.2,57.3) **
HEMODYNAMIC PARAMETERS					
MAP	SS	75 (67,82)	58 (46,70) °°	68 (64,74)	71 (69,72)
	SH	80 (73,86)	73 (70,78)	74 (66,82)	73 (68,76)
SAP	SS	103 (93,107)	72 (64,95) °°	100 (90,107)	99 (94,102)
	SH	103 (97,110)	100 (96,107) *	104 (97,106)	99 (92,106)
DAP	SS	57 (51,63)	43 (34,52) °°	45 (41,53) °	51 (48,53)
	SH	58 (56,67)	56 (49,59)	52 (47,59)	54 (49,54)
HR	SS	112 (108,117)	177 (171,214) °	170 (150,176) °	144 (113,150)
	SH	97 (94,118)	85 (78,96) *	68 (56,74) *	53 (50,66) *°
ABF	SS	188 (148,206)	108 (100,119)	222 (175,237) ##	182 (177,226) ##
	SH	180 (170,202)	179 (164,185) **	206 (159,232)	188 (177,206)

N%: band neutrophils [%], Hb: hemoglobin [g/L], Htc: hematocrit [L/L], Lact: lactate [mmol/L], SvO_2: mixed venous oxygen saturation [%], MAP: mean arterial pressure [mmHg], SAP: systolic arterial pressure [mmHg], DAP: diastolic arterial pressure [mmHg], HR: heart rate [bpm], ABF arterial blood flow [mL/min], SS: septic pigs, SH: sham pigs, T1: baseline, T2: after sepsis development, T3: after 24h of resuscitation, T4: after 48h of resuscitation. Comparison between Sepsis and Sham: *p-value < 0.05, **p-value < 0.01 (Wilcoxon rank sum test, between groups). Wilcoxon signed test: °p < 0.05 with respect to T1, #p < 0.05 with respect to T2, ##p < 0.01 with respect to T2, §p < 0.05 with respect to T3 (Friedman test p-value < 0.05). The number reported in the apex refers to the number of pigs with available data, if not all.

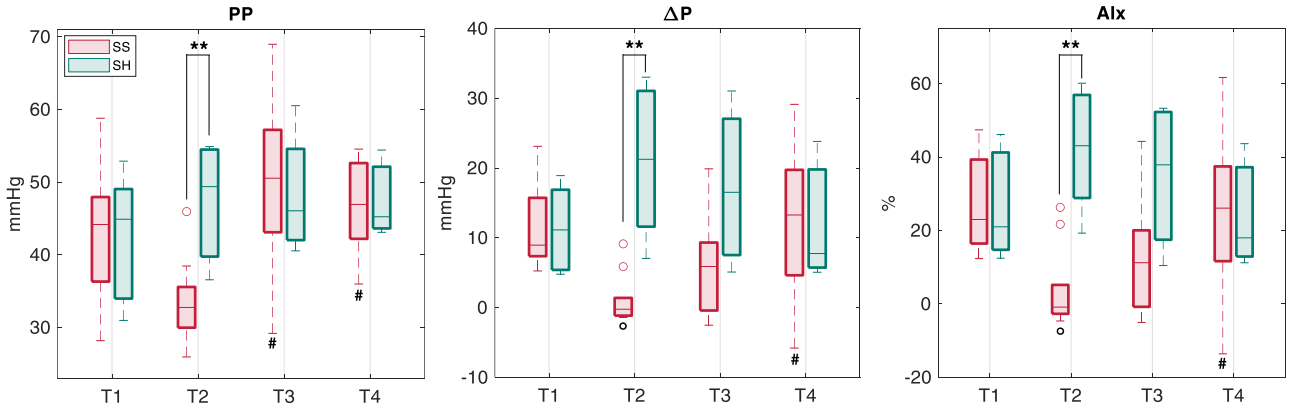

Fig. 3. Boxplots of pulse wave indices for both populations at each time point. Panel A: boxplot of pulse pressure (PP) values; Panel B: boxplot of augmented pressure (ΔP) values; Panel C: boxplot of augmentation index (AIx) values. T1: baseline; T2: after sepsis development; T3: after 24h of resuscitation; T4: after 48h of resuscitation. Wilcoxon signed test: °p<0.05 with respect to T1 #p-value<0.05 with respect to T2 (Friedman test p-value<0.05). Wilcoxon rank sum test: **p<0.01 between the two groups at specific time point.

C. *Input and characteristic impedance*

The Bland-Altman and the correlation analyses between the different estimates of *Zc* are reported in the supplementary materials. The measures showed a strong agreement (ρ=0.9 between the two time domain estimates, p-value<10^{-3}; ρ=0.8 between the time domain and the frequency domain estimates, p-value<10^{-3}), highlighting the robustness of the methods and the reliability of the estimates.

Fig. 4 shows the distribution of values of characteristic impedance *Zc* computed by applying the Fourier series decomposition. Sepsis induced an increase in *Zc*, reaching values significantly higher than SH pigs. During resuscitation, *Zc* values gradually decreased to values similar to baseline and SH pigs.

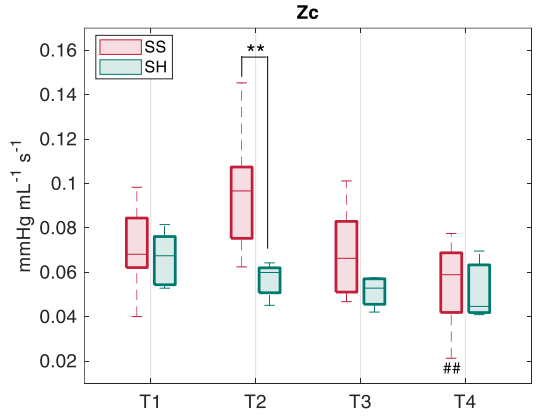

Fig. 4: Boxplot of characteristic impedance (Zc) values derived with Fourier analysis for both populations at each time point. T1: baseline; T2: after sepsis development; T3: after 24h of resuscitation; T4: after 48h of resuscitation. Wilcoxon signed test: ##p-value<0.01 with respect to T2 (Friedman test p-value<0.05). Wilcoxon rank sum test: **p<0.01 between the two groups at specific time point.

Fig. 5 and Fig. 6 illustrate the trend of *Zin* modulus and phase at each time point, respectively. At baseline (T1) the trend of *Zin* was very similar in the two populations, and it showed the typical characteristics of type A pulse [27], i.e., the modulus decreases steeply after the component *k*=0, which represents the peripheral resistance to average flow, reaching a minimum around the 3rd or 4th harmonic; after this point the modulus increases gradually up to a local maximum and then it starts to oscillate. The phase spectrum shows negative values in the first harmonics, hinting that flow leads pressure; afterwards, it typically shows a cross-over from negative to positive values at the harmonic corresponding to the minimum of *Zin* modulus, which is also called *critical frequency*; after this frequency the phase is expected to stay close to zero. A near zero phase at higher frequencies indicates cancellation of in- and out-of-phase incident and reflected waves, and, therefore, the associated impedance modulus is expected to oscillate around the value of characteristic impedance *Zc* [31]. Fluctuations in *Zin* modulus and phase are due to wave reflections [33]. After sepsis development (T2) significant differences were observed in the values between the two groups, mostly in the first harmonics. SS group demonstrated a flatter modulus in the first six harmonics compared to SH group, who, on the contrary, showed features similar to baseline. Moreover, the values of *Zin* modulus at the first harmonic were lower at T2 compared to T1 in SS pigs (T1: 0.17 (0.11, 0.19) T2: 0.10 (0.07, 0.11), p-value < 0.002, Wilcoxon signed test).

Moreover, SS pigs showed values of the phase very close to zero, and the zero-crossing point was between the 1st and the 2nd harmonic, i.e. some harmonics sooner than at T1. These patterns are consistent with type B or C waveform, i.e. a simpler system with reduced reflections which requires fewer harmonics to be described in the frequency domain. For this reason, the harmonics higher than 5 were not used for *Zc* computation. High values of modulus and phase at these harmonics may be due to noise and artefacts and not to the signal's content.

Interestingly, significant differences in *Zin* modulus and phase between SS and SH pigs were observed also at T3 and T4, mostly in the first harmonics, despite the overall trend of values was resembling the baseline trend. This suggests that an impairment of wave reflection phenomena may persist, as confirmed by the indices reported in the follow.

D. *Wave reflection and waveform complexity indices*

Fig. 7 shows the values distribution of wave reflection indices (RM, RI, normalized *Zin*) computed at each time point.

The trend of all indices was very similar, i.e., it showed a significant decrease at T2, in agreement with a condition of less reflections, as highlighted before; afterwards, the indices showed gradually increasing values, but without reaching values similar to sham pigs, although only *Zin* normalized values showed statistical significance.

HD showed a consistent trend with the previous indices, supporting the idea that the complexity of the arterial waveform is related to wave reflections.

E. Wave separation analysis

Fig. 8 shows examples of the forward and reflected waves in one septic pig at all time points. Table IV reports the values of the indices for the same pig. At T1 a highly pronounced inflection point is clear during the systolic rising (type A waveform) and corresponds to the onset of the backward wave and the ABF peak, consistently with the physiology. After sepsis development at T2, the waveform changed to type B or C in almost all animals, and the backward pressure wave appeared much flatter compared to T1, suggesting less reflection phenomena. As a consequence, the forward wave at T2 is very similar to the measured ABP waveform, representing indeed its major contribution. At T2 the amplitude of the backward wave is significantly decreased in septic pigs compared to sham pigs (Table III and Fig. 5S); the wave reflection transit time (Tr), i.e., the time of arrival of Pb, is longer, although not statistically significant, in septic pigs with respect to sham pigs (Table III and Fig. 6S), confirming the reduced contribution of total wave reflection on the overall ABP wave morphology. The amplitude of backward wave gradually increased again after T3 and Tr gradually decreased, despite some differences with baseline condition can still be observed, e.g., the end of ejection occurred later in the beat.

The amplitude values of forward and backward waves and the wave reflection transit time Tr are reported in Table III and in Fig. 5S and Fig. 6S in the supplementary materials.

TABLE III
MEDIAN (25TH-75TH PERCENTILES) VALUES OF AMPLITUDE OF FORWARD AND BACKWARD WAVE AND WAVE REFLECTION TRANSIT TIME

		T1	T2	T3	T4
Pb	SS	14 (11,17)	7 (7,9) °	11 (9,17)	16 (14,18) ##
	SH	15 (14,17)	17 (15,23) **	16 (15,21)	17 (16,23)
Pf	SS	32 (26,35)	32 (29,37)	43 (37,46)	33 (28,41)
	SH	33 (23,34)	33 (27,35)	31 (27,37)	33 (30,35)
Tr	SS	90 (88,123)	130 (90,150)	90 (90,120)	95 (85,100)
	SH	100 (88,103)	100 (98,103)	100 (95,115)	90 (90,105)

Pb: backward pressure wave amplitude [mmHg], Pf: forward pressure wave amplitude [mmHg], Tr: wave reflection transit time [ms]. SS: septic pigs, SH: sham pigs, T1: baseline, T2: after sepsis development, T3: after 24h of resuscitation, T4: after 48h of resuscitation. Wilcoxon signed test: °p<0.05 with respect to T1, ## p<0.01 with respect to T2 (Friedman test p-value<0.05). Wilcoxon rank sum test: **p<0.01 between the two groups at specific time point.

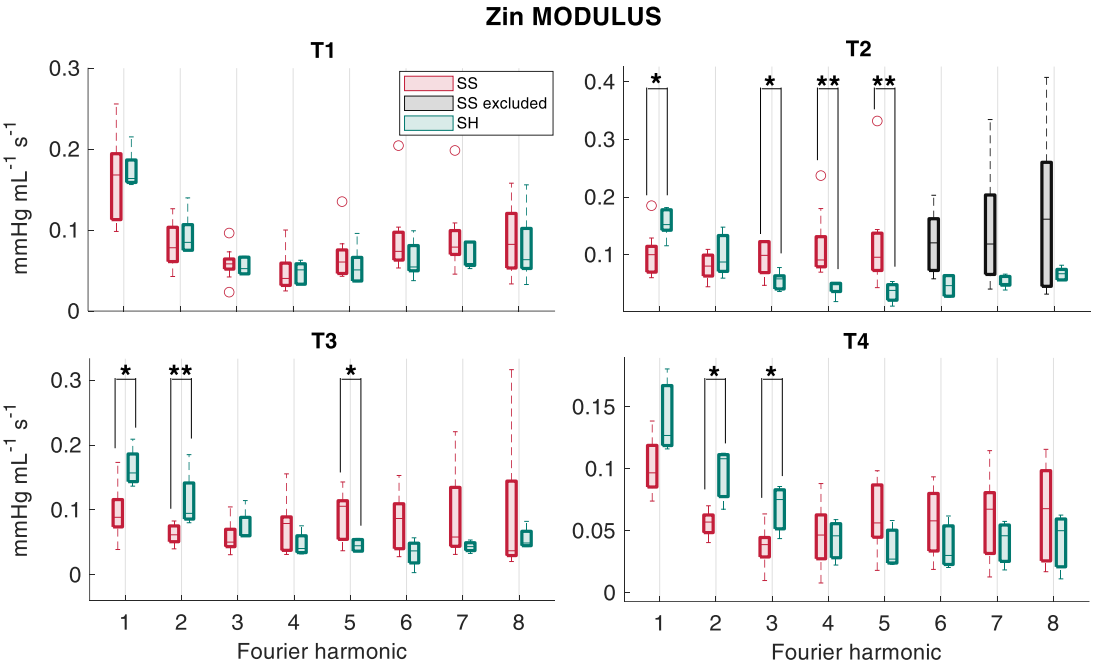

Fig. 5. Boxplot of input impedance (Zin) modulus values derived with Fourier analysis for both populations at each time point. T1: baseline; T2: after sepsis development; T3: after 24h of resuscitation; T4: after 48h of resuscitation. Wilcoxon rank sum test: *p<0.05, **p<0.01 between the two groups at specific harmonic. Fourier harmonic are multiple of the fundamental frequency $f_0=1/T_0$ where T_0 is the beat duration. Grey boxplots represent harmonics excluded: in septic shock condition, we observed the typical "bell-shape" type B waveform, which is a much simpler waveform that can be described with fewer coefficients; the high values of modulus and phase at these harmonics may be due to noise and artefacts and not to the signal's content.

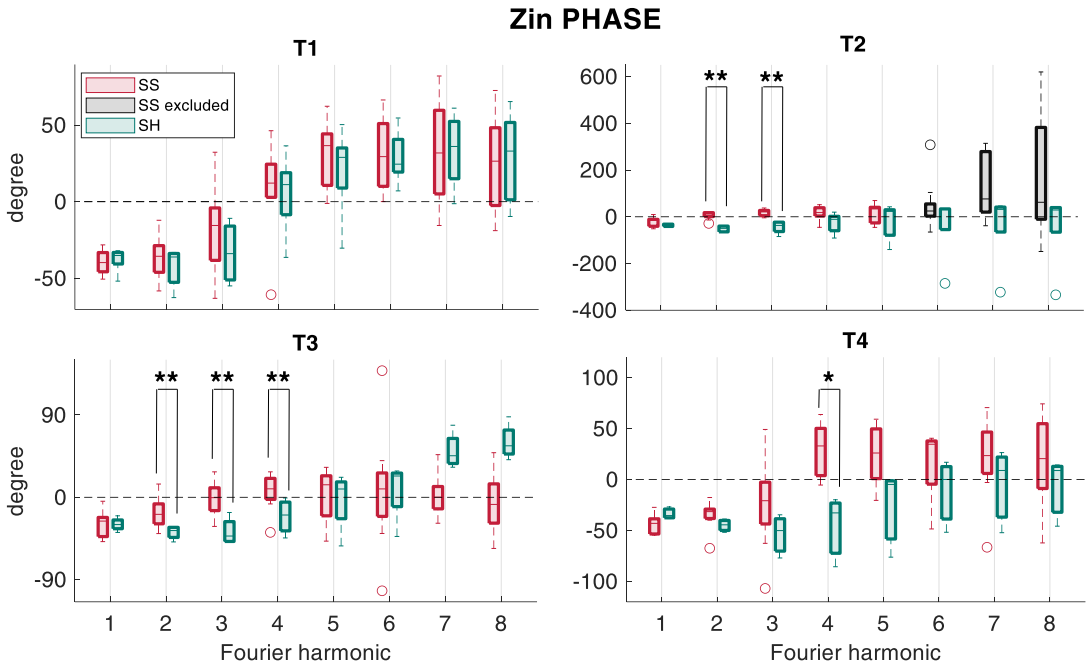

Fig. 6. Boxplot of input impedance (Zin) phase values derived with Fourier analysis for both populations at each time point. T1: baseline; T2: after sepsis development; T3: after 24h of resuscitation; T4: after 48h of resuscitation. Wilcoxon rank sum test: *p<0.05, **p<0.01 between the two groups at specific harmonic. Fourier harmonic are multiple of the fundamental frequency $f_0=1/T_0$ where T_0 is the beat duration. Grey boxplots represent harmonics excluded: in septic shock condition, we observed the typical "bell-shape" type B waveform, which is a much simpler waveform that can be described with fewer coefficients; the high values of modulus and phase at these harmonics may be due to noise and artefacts and not to the signal's content..

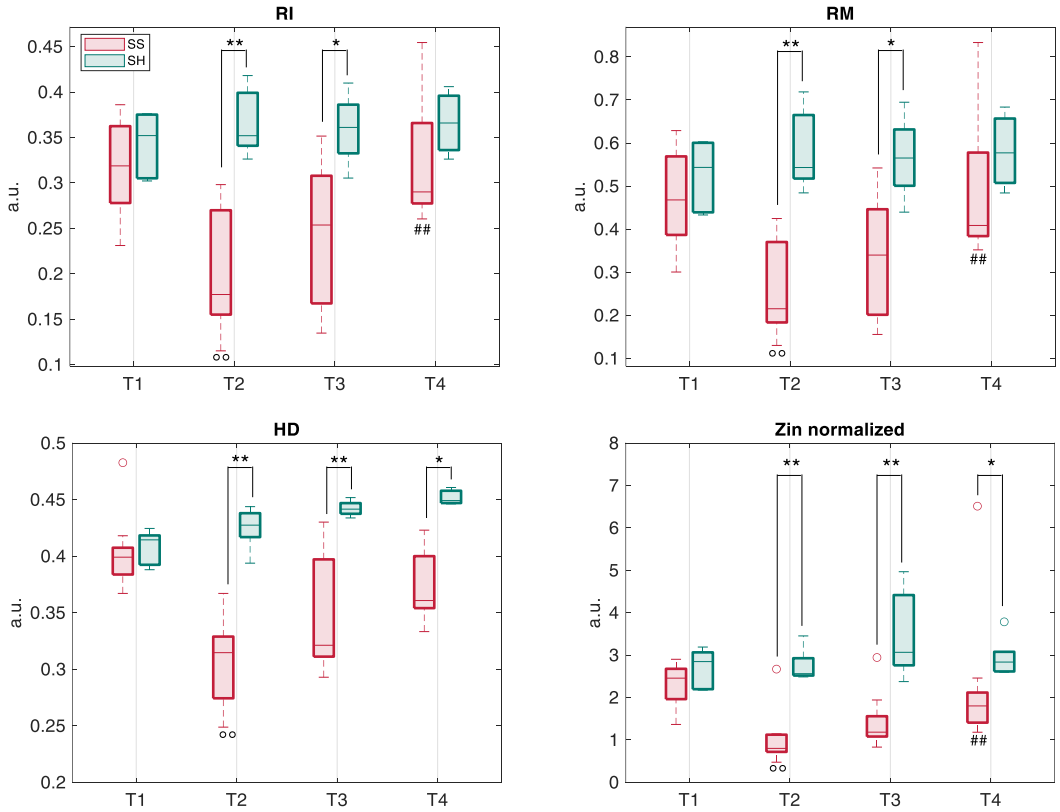

Fig. 7. Boxplot of waveform complexity (HD) and wave reflection (RM, RI, Zin normalized) indices for both populations at each time point. T1: baseline; T2: after sepsis development; T3: after 24h of resuscitation; T4: after 48h of resuscitation. Wilcoxon signed test: ° p<0.05, °°p<0.01 with respect to T1, ##p<0.01 with respect to T2 (Friedman test p-value<0.05). Wilcoxon rank sum test: *p<0.05, **p<0.01 between the two groups at specific time point.

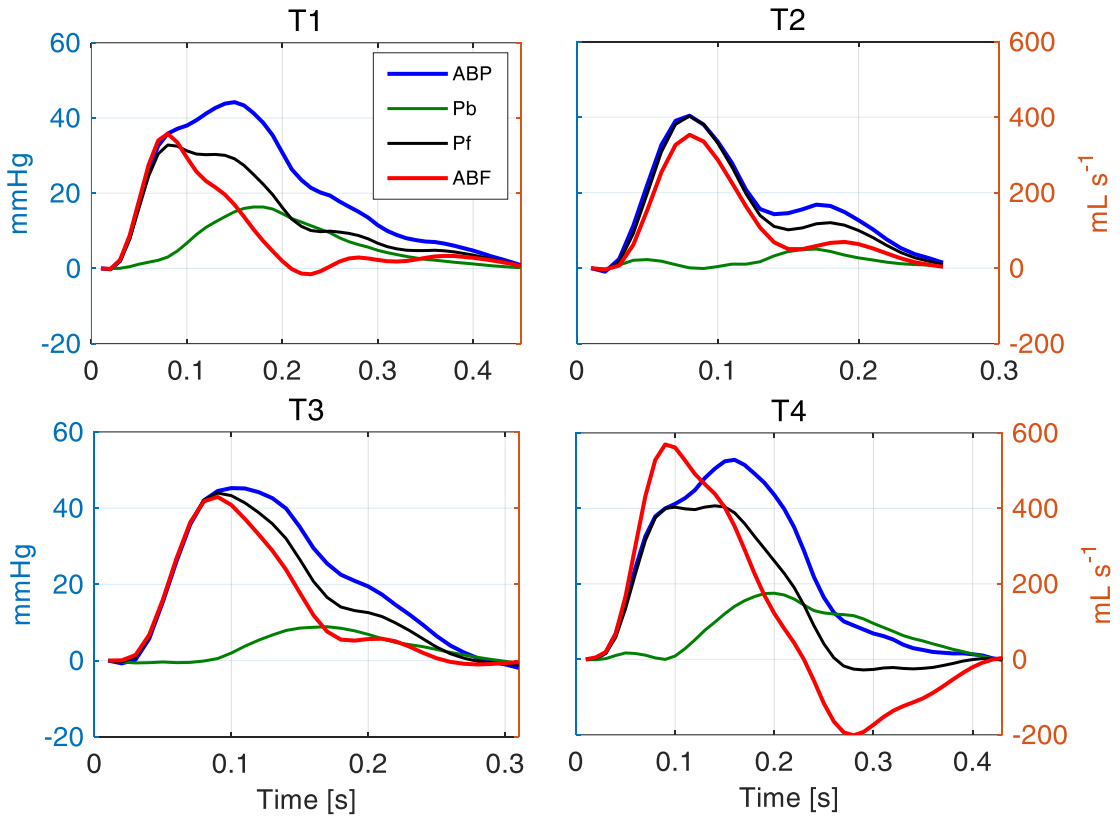

Fig.8. Examples of forward (Pf, black line) and backward (Pb, green line) arterial blood pressure (ABP, blue line) waves computed in one septic pig at each time point of the experiment. All the signals are displayed so to start from 0 to highlight the amplitude ratios. ABF: arterial blood flow (red line); T1: baseline; T2: after sepsis development; T3: after 24h of resuscitation; T4: after 48h of resuscitation.

TABLE IV
VALUES OF THE INDICES AT EACH TIME POINT FOR THE SEPTIC PIG REPRESENTED IN FIG. 8

	SAP	DAP	MAP	PP	ABF	AIx	Zc	Pb	Pf	Tr	RI	RM	Zin norm	HD
T1	104	57	77	48	136	18.8	0.08	16.4	33	0.08	0.33	0.5	2	0.4
T2	94	48	67	46	120	-2.5	0.11	5.3	41	0.13	0.12	0.13	0.8	0.25
T3	92	42	66	50	159	15.2	0.1	9.6	45	0.09	0.18	0.21	1.2	0.29
T4	105	53	75	52	194	32	0.07	17.7	43	0.1	0.29	0.41	1.2	0.36

SAP: systolic arterial pressure [mmHg], DAP: diastolic arterial pressure [mmHg], MAP: mean arterial pressure [mmHg], PP: pulse pressure [mmHg], ABF: mean arterial blood flow [mL/s], AIx: augmentation index [%], Zc: characteristic impedance [mmHg/mL/s], Pb: backward wave amplitude [mmHg], Pf: forward wave amplitude [mmHg], Tr: backward wave transit time [s], RI: reflection index [a.u.], RM: reflection magnitude [a.u.], Zin norm: normalized input impedance [a.u.], HD: harmonic distortion [a.u.]

IV. DISCUSSION

The primary objective of this study was to test the feasibility of applying PWA and wave separation techniques to investigate the changes induced by polymicrobial sepsis in ABP waveform morphology and wave reflection in a swine population, and to explore how standard clinical resuscitation according to guidelines was effective in restoring a physiological ABP wave transmission and reflection during a long-term resuscitation window of 72 hours.

In our protocol ABP and ABF were collected at the carotid arterial site, since this has been used in the original publication [25] – aortic signals were therefore not available for this study. Nevertheless, carotid artery pressure is often used as a surrogate for central artery or aortic pressure because of the close proximity of these arterial sites [37], [38]. In addition, the carotid artery is the main vessel responsible for oxygen delivery to the brain tissue, and pathological changes of the carotid artery and consequent alterations in pulse wave propagation and reflection can have an impact on the brain microcirculation due to an altered pulsatility dampening [39], [40]. Carotid pulse wave analysis has also been shown to be a valuable tool for hemodynamic and cardiovascular risk assessment [41]. Therefore, carotid artery may convey important information that can explain septic shock patients' outcome.

A. *Effects of sepsis on wave morphology and reflection*

The results demonstrated that sepsis induced a great alteration in carotid ABP waveform, changing from a type A to

a type B or C. Type B beats are typical of a system with little or more diffuse reflections, showing very small secondary rises in systolic pressure [34]. Accordingly, ΔP and PP were significantly reduced at T2 in septic pigs and AIx reached negative values in almost all pigs (Fig. 3). Moreover, all the indices computed to quantify wave reflections, i.e., RM, RI, and normalized Zin, supported the evidence of reduced reflections following sepsis development, as they were significantly reduced in septic animals at T2 (Fig. 7); the amplitude of the backward wave was also significantly decreased at T2 in SS pigs compared to SH pigs and baseline values (Table III). However, the tachycardia in septic animals at T2 may have affected AIx values, as it is known that increased HR leads to a reduced AIx [42].The values of HD were significantly reduced at T2, consistently with the hypothesis that an overall decrease in wave reflections produce a simpler arterial waveform, i.e., a bell-shaped type B waveform. Although HD is an index principally used in the context of electrical and telecommunication engineering, it has recently gained attention also in the field of hemodynamics [35], [36], [43], where it has been proposed as a surrogate index of arterial stiffness, despite further evidence is still necessary to make conclusions. In this work we hypothesize that HD can be related to the amount of wave reflection, since a ABP waveform consisting of fewer reflected waves should be a "simpler" waveform and assume lower values of HD index according to its mathematical meaning. Our results show how HD trend is highly comparable with the trends of RM and RI values, indexes more widely accepted as markers of wave reflection, thus supporting the use of HD index in this context. Moreover, in terms of computational complexity, we can observe that RM and RI indexes require the estimation of characteristic impedance, the availability of blood flow measure, the estimation of forward and backward wave, and, finally, the estimation of forward and backward wave amplitude. On the contrary HD computation is based solely on the Fourier series decomposition of the arterial blood pressure waveform; the ease of HD computation aroused interest to investigate if it is associated to RM and RI and thus conveys similar information.

In septic pigs *Zin* modulus and phase values at T2 are consistent with type B or C waveforms [18], e.g. the values of *Zin* modulus at the first harmonic are lower than baseline, and the critical frequency occurred early (i.e., the frequency were the modulus crosses the zero value), as already discussed in details in the results section.

We can hypothesize that the severe peripheral vasodilation that is known to occur during sepsis and septic shock [44], is responsible for the decrease in wave reflections, as also previously reported by other studies [45], [46]. Indeed, the incident pulse wave generated by the left ventricle travels away along the arterial tree and it is partially reflected at vascular bifurcations or arterial-arteriolar impedance mismatches (e.g. vascular tapering) [26]. In a previous study on the same animal population the authors found that the compliance of the carotid vessel was highly reduced by sepsis development [12]; therefore, we can also hypothesize that the stiffening of large arteries, such as the aorta or carotid artery, may reduce the degree of impedance mismatch between central and distal vessels, leading to a more well matched arterial system and thus a system with fewer wave reflections.

In support of this second hypothesis, we can observe that the value of *Zc* at T2 was significantly larger in SS pigs compared to SH pigs. We know that *Zc* depends on blood density (ρ), wave velocity (c) and the vessel's cross-sectional area (A) according to the following equation:

$$Z_c = \frac{\rho c}{A} \quad [\mathrm{dyn} * \mathrm{s} * cm^{-5}] \tag{12}$$

The carotid stiffening can have played a crucial role in Zc increase following sepsis, since a stiffer vessel typically leads to an increase in wave velocity c; moreover, the blood density due to capillary leakage is also increased as the increased hematocrit values of SS pigs at T2 confirm (Table II). Multiple mechanisms potentially underlie increased arterial stiffness during sepsis, encompassing both functional and structural changes, such as alteration in collagen metabolism [47], changes in endothelial permeability resulting in tissue edema, and other changes in the interstitial matrix [48]. Functional changes include endothelial dysfunction and abnormal vasoconstrictor responses [49], [50].

B. Effects of resuscitation on wave morphology and reflection

The administration of therapy was successful in restoring MAP and SvO_2 to physiologic values according to the current guidelines (Table II). However, the recovering of mean hemodynamic values may not imply the return to a physiological condition of the cardiovascular system, as already highlighted by previous experimental results [11], [12], [51]. In support of this, wave reflection indices remained lower in SS pigs compared to SH pigs after 48 h of resuscitation (Fig. 7), although not significantly except for *Zin normalized*, supporting the idea that the alterations in wave reflections were still present. Moreover, the trends in *Zin* modulus and phase are different between the two populations still at T3 and T4 mainly in the first harmonics (Fig. 5 and Fig. 6).

The non-significant differences in amplitude of forward and backward waves between the two populations and among the time points of the experiment may be related to the fact that the reflected wave is a composite wave consisting of many individual waves resulting from the many reflection sites in the arterial system [26].

HD was still significantly reduced in SS pigs compared to SH pigs at T4, strengthening the evidence of persistent alterations of wave reflection as emerged from the wave reflection indices previously described.

Zc of SS pigs returned to values similar to T1 and SH pigs at the end of resuscitation (T4), although we demonstrated previously in the same group of animals, that the carotid compliance was still significantly lower than SH animals both at T3 and T4 [12].

The values of ΔP and AIx gradually increased to reach values very similar to baseline after resuscitation although the high variability in SS pigs, mainly at T4, highlighted the large inter-

subject variability in the response to resuscitation, similarly to the clinical scenario. We must recall however that AIx index is a composite index affected by many factors other than changes in wave reflections due to vascular alterations [9], [52]. For example, a negative relationship between HR and AIx is well known [42], [52], a positive relationship between left ventricular contraction velocity and AIx has been described as well [9]. Finally, the administration of noradrenaline, which is the first line vasopressor recommended in clinics, has been shown to strongly influence AIx in patients with septic shock [53]; in particular, the higher the noradrenaline dosage the higher the AIx and the higher is the ventricular afterload, thus impacting the heart functionality. For these reasons, AIx values and trends have to be carefully interpreted in the context of critical illness, such as in sepsis, where all these factors may change at the same time.

The prolonged impairment of blood propagation and reflection, persisting even after 48 hours of hemodynamic stabilization in septic pigs, is typically induced by structural and functional changes of arterial vascular properties, that lead to non-physiological impedance mismatches and, consequently, alterations in pressure and flow wave reflections [39]. Indeed, in a previous work, our group found a persistent stiffness of the carotid vessel and a peripheral vasodilation despite adequate resuscitation [12]. Wave reflection at the junction between the highly compliant aorta and relatively stiffer peripheral arteries represents a protective mechanism that limits transmission of excessive pulsatility into the microcirculation [39], e.g., from the carotid artery into the brain microcirculation. Indeed, the pulsatile flow transmits through the arterial system until it reaches the microvascular beds, where it is largely damped, resulting in relatively continuous venous flow. This process, known as pulsatility damping, has important physiological implications for microvascular function [54]. In the arterioles, cyclic stretch and shear stress induced by pulsatile flow constitute important regulators of vascular endothelial functions, such as the release of nitric oxide (NO). The low pulsatility in capillaries and venules protects organs by ensuring continuous oxygen supply to the tissue. On the opposite, a penetration of pulsatility into capillaries and venules may impair vascular function such as that of the brain microvascular endothelium [40], [55]. Alterations in the propagation of arterial wave could help to understand the potential mechanisms underlying the well-known long-term cardiovascular complications that affect many of survived septic patients [21], [22].

C. Limitations of the study

The main limitation of this study is the reduced sample size of the animal population that, combined to the physiological heterogeneity in the individual response to sepsis resuscitation, may have affected the statistical significance of the indices values and trends. Moreover, the animals were observed for a limited time window (i.e., 48 hours) and many of these alterations may vanish later on. However, the short-term response is known to be particularly crucial for the long-term outcome of the patient [7], [21], thereby our indices are still valid to optimize the acute phase of therapy administration.

Another limitation is the different sites of registration of pressure and flow waveforms (i.e., left and right carotid artery, respectively) eventually causing asynchronization of the two signals that had to be carefully corrected during the preprocessing stage, as described in the Methods section.

Moreover, the use of carotid pressure and flow signals instead of the more central aortic registrations prevent to draw conclusions about the impact of wave reflections at the level of the heart and to extrapolate information on peripheral vascular changes other than the brain, that is the main “afterload” of the carotid artery.

Finally, the measure of blood flow is typically invasive or not commonly available in patients, e.g. echo doppler examinations are not routinely performed for this purpose. However, several approaches have been proposed to model flow from the measurement of arterial waveform, for example the triangular approximation or its modifications [56]. In the work of Manoj et al. wave separation analysis has been obtained by decomposing the carotid ABP waveform into Gaussians without the use of flow measures [57]. These methods have been primarily tested on healthy subjects, simulated data or chronic patients, they should be adapted and tested to work properly also in a complex condition as in critically ill patients.

V. CONCLUSION

In conclusion, the presented results highlighted that the resuscitation protocol was not able to restore a physiological condition of blood propagation and reflection, despite it can be considered effective according to standard clinical targets. In particular, the amount of reflected waves was found to be still significantly reduced in the septic population even after 48 hours of hemodynamic stabilization. These persistent alterations could help to understand the potential mechanisms underlying the well-known long-term cardiovascular complications that affect many of survived septic patients [21], [22]. Whether the proposed indices (RM, RI, HD, normalized Zin) have a direct relation with long-term outcome in patients is still to be determined, but their potential use could be enormous in the clinical practice, for example, in the setting of therapy response monitoring: if the administered therapy does result in a continuous worsening of wave reflection phenomena this could be read as a marker of harm for the patient since this condition could impair the end-organs microcirculation. This could trigger alternative, personalized resuscitation strategies.

REFERENCES

[1] D. C. Angus, “The lingering consequences of sepsis: A hidden public health disaster?,” *Jama*, vol. 304, no. 16, pp. 1833–1834, 2010, doi: 10.1001/jama.2010.1546.

[2] Y. Sakr *et al.*, “Sepsis in intensive care unit patients: Worldwide data from the intensive care over nations audit,” *Open Forum Infect. Dis.*, vol. 5, no. 12, pp. 1–9, 2018, doi: 10.1093/ofid/ofy313.

[3] K. E. Rudd *et al.*, “Global, regional, and national sepsis incidence and mortality, 1990–2017: analysis for the Global Burden of Disease Study,” *Lancet*, vol. 395, no.

10219, pp. 200–211, 2020, doi: 10.1016/S0140-6736(19)32989-7.

[4] E. C. van der Slikke, A. Y. An, R. E. W. Hancock, and H. R. Bouma, "Exploring the pathophysiology of post-sepsis syndrome to identify therapeutic opportunities," *EBioMedicine*, vol. 61, p. 103044, 2020, doi: 10.1016/j.ebiom.2020.103044.

[5] A. J. Goodwin, D. A. Rice, K. N. Simpson, and D. W. Ford, "Frequency, cost, and risk factors of readmissions among severe sepsis survivors," *Crit. Care Med.*, vol. 43, no. 4, pp. 738–746, 2015, doi: 10.1097/CCM.0000000000000859.

[6] G. Rawal, S. Yadav, and R. Kumar, "Post-intensive care syndrome: An overview," *J. Transl. Intern. Med.*, vol. 5, no. 2, pp. 90–92, 2017, doi: 10.1515/jtim-2016-0016.

[7] L. Evans *et al.*, "Surviving sepsis campaign: international guidelines for management of sepsis and septic shock 2021," *Intensive Care Med.*, vol. 47, no. 11, pp. 1181–1247, 2021, doi: 10.1007/s00134-021-06506-y.

[8] K. S. Heffernan, E. A. Patvardhan, M. Hession, J. Ruan, R. H. Karas, and J. T. Kuvin, "Elevated augmentation index derived from peripheral arterial tonometry is associated with abnormal ventricular-vascular coupling," *Clin. Physiol. Funct. Imaging*, vol. 30, no. 5, pp. 313–317, 2010, doi: 10.1111/j.1475-097X.2010.00943.x.

[9] M. H. G. Heusinkveld *et al.*, "Augmentation index is not a proxy for wave reflection magnitude: Mechanistic analysis using a computational model," *J. Appl. Physiol.*, vol. 127, no. 2, pp. 491–500, 2019, doi: 10.1152/japplphysiol.00769.2018.

[10] W. W. Nichols, M. F. O'Rourke, and C. Vlachopoulos, *McDonald's Blood Flow in Arteries Theoretical, Experimental and Clinical Principles*, 6th ed. CRC Press, 2011.

[11] M. Carrara, A. Herpain, G. Baselli, and M. Ferrario, "Vascular Decoupling in Septic Shock: The Combined Role of Autonomic Nervous System, Arterial Stiffness, and Peripheral Vascular Tone," *Front. Physiol.*, vol. 11, no. July, pp. 1–13, 2020, doi: 10.3389/fphys.2020.00594.

[12] M. Carrara *et al.*, "Autonomic and circulatory alterations persist despite adequate resuscitation in a 5-day sepsis swine experiment," *Sci. Rep.*, vol. 12, no. 1, pp. 1–14, 2022, doi: 10.1038/s41598-022-23516-y.

[13] S. Kazune, A. Grabovskis, C. Cescon, E. Strike, and I. Vanags, "Association between increased arterial stiffness and clinical outcomes in patients with early sepsis: a prospective observational cohort study," *Intensive Care Med. Exp.*, vol. 7, no. 1, 2019, doi: 10.1186/s40635-019-0252-3.

[14] C. Vlachopoulos *et al.*, "Acute systemic inflammation increases arterial stiffness and decreases wave reflections in healthy individuals," *Circulation*, vol. 112, no. 14, pp. 2193–2200, 2005, doi: 10.1161/CIRCULATIONAHA.105.535435.

[15] M. Carrara, A. Niccolo, A. Herpain, and M. Ferrario, "Reducing tachycardia in septic shock patients: Do esmolol and ivabradine have a chronotropic effect only?," *Proc. Annu. Int. Conf. IEEE Eng. Med. Biol. Soc. EMBS*, vol. 2020-July, pp. 382–385, 2020, doi: 10.1109/EMBC44109.2020.9176309.

[16] F. Hatib, J. R. C. Jansen, and M. R. Pinsky, "Peripheral vascular decoupling in porcine endotoxic shock," *J. Appl. Physiol.*, vol. 111, no. 3, pp. 853–860, 2011, doi: 10.1152/japplphysiol.00066.2011.

[17] T. S. Phan *et al.*, "Aging is Associated With an Earlier Arrival of Reflected Waves Without a Distal Shift in Reflection Sites," *J. Am. Heart Assoc.*, vol. 5, no. 9, 2016, doi: 10.1161/JAHA.116.003733.

[18] J. A. Chirinos *et al.*, "Arterial wave reflections and incident cardiovascular events and heart failure: MESA (Multiethnic Study of Atherosclerosis)," *J. Am. Coll. Cardiol.*, vol. 60, no. 21, pp. 2170–2177, 2012, doi: 10.1016/j.jacc.2012.07.054.

[19] G. F. Mitchell *et al.*, "Changes in arterial stiffness and wave reflection with advancing age in healthy men and women: The Framingham Heart Study," *Hypertension*, vol. 43, no. 6, pp. 1239–1245, 2004, doi: 10.1161/01.HYP.0000128420.01881.aa.

[20] J. I. Davies and A. D. Struthers, "Beyond blood pressure: pulse wave analysis – a better way of assessing cardiovascular risk?," *Future Cardiol.*, vol. 1, no. 1, pp. 69–78, 2005, doi: 10.1517/14796678.1.1.69.

[21] H. Merdji *et al.*, "Septic shock as a trigger of arterial stress-induced premature senescence: A new pathway involved in the post sepsis long-term cardiovascular complications," *Vascul. Pharmacol.*, vol. 141, no. September, 2021, doi: 10.1016/j.vph.2021.106922.

[22] H. Merdji, V. Schini-Kerth, F. Meziani, and F. Toti, "Long-term cardiovascular complications following sepsis: is senescence the missing link?," *Ann. Intensive Care*, vol. 11, no. 1, 2021, doi: 10.1186/s13613-021-00937-y.

[23] M. Ferrario *et al.*, "Persistent hyperammonia and altered concentrations of urea cycle metabolites in a 5-day swine experiment of sepsis," *Sci. Rep.*, vol. 11, no. 1, pp. 1–13, 2021, doi: 10.1038/s41598-021-97855-7.

[24] S. Liu *et al.*, "Defense mechanisms to increasing back pressure for hepatic oxygen transport and venous return in porcine fecal peritonitis.," *Am. J. Physiol. Gastrointest. Liver Physiol.*, vol. 319, no. 3, pp. G289–G302, Sep. 2020, doi: 10.1152/ajpgi.00216.2020.

[25] S. Liu *et al.*, "Defense mechanisms to increasing back pressure for hepatic oxygen transport and venous return in porcine fecal peritonitis," *Am. J. Physiol. - Gastrointest. Liver Physiol.*, vol. 319, no. 3, pp. G289–G302, 2020, doi: 10.1152/ajpgi.00216.2020.

[26] N. Westerhof and B. E. Westerhof, "Wave transmission and reflection of waves ' The myth is in their use,'" *Artery Res.*, vol. 6, no. 1, pp. 1–6, 2012, doi: 10.1016/j.artres.2012.01.004.

[27] W. W. Nichols, C. R. Conti, W. E. Walker, and W. R. Milnor, "Input impedance of the systemic circulation in man," *Circ. Res.*, vol. 40, no. 5, pp. 451–458, 1977, doi: 10.1161/01.RES.40.5.451.

[28] N. Westerhof, P. Sipkema, G. C. V. Den Bos, and G. Elzinga, "Forward and backward waves in the arterial

system," *Cardiovasc. Res.*, vol. 6, no. 6, pp. 648–656, 1972, doi: 10.1093/cvr/6.6.648.

[29] W. Zong, T. Heldt, G. B. Moody, and R. G. Mark, "An open-source algorithm to detect onset of arterial blood pressure pulses," *Comput. Cardiol. 2003*, pp. 259–262, 2003, doi: 10.1109/CIC.2003.1291140.

[30] M. Karamanoglu, "A system for analysis of arterial blood pressure waveforms in humans," *Comput. Biomed. Res.*, vol. 30, no. 3, pp. 244–255, 1997, doi: 10.1006/cbmr.1997.1450.

[31] M. U. Qureshi *et al.*, "Characteristic impedance: Frequency or time domain approach?," *Physiol. Meas.*, vol. 39, no. 1, 2018, doi: 10.1088/1361-6579/aa9d60.

[32] J.-P. L. Dujardin and D. N. Stone, "Characteristic impedance of the proximal aorta determined in the time and frequency domain: a comparison," *Med Biol Eng Comput.*, vol. 19, no. September, pp. 565–568, 1981.

[33] B. M. F. O. Rourke and M. G. Taylor, "Input Impedance of the Systemic Circulation," *Circ. Res.*, vol. XX, no. 4, pp. 365–380, 1967.

[34] J. P. Murgo, N. Westerhof, J. P. Giolma, and S. A. Altobelli, "Aortic input impedance in normal man: Relationship to pressure wave forms," *Circulation*, vol. 62, no. 1, pp. 105–116, 1980, doi: 10.1161/01.CIR.62.1.105.

[35] N. Milkovich, A. Gkousioudi, F. Seta, B. Suki, and Y. Zhang, "Harmonic Distortion of Blood Pressure Waveform as a Measure of Arterial Stiffness," *Front. Bioeng. Biotechnol.*, vol. 10, no. March, pp. 1–11, 2022, doi: 10.3389/fbioe.2022.842754.

[36] Y. J. Park, J. M. Lee, and K. H. Choi, "Harmonic components of photoplethysmography and pathological patterns: A cross-sectional study," *Medicine (Baltimore).*, vol. 102, no. 35, p. e34200, 2023, doi: 10.1097/MD.0000000000034200.

[37] C. M. McEniery, J. R. Cockcroft, M. J. Roman, S. S. Franklin, and I. B. Wilkinson, "Central blood pressure: Current evidence and clinical importance," *Eur. Heart J.*, vol. 35, no. 26, pp. 1719–1725, 2014, doi: 10.1093/eurheartj/eht565.

[38] V. Bikia, G. Rovas, S. Anagnostopoulos, and N. Stergiopulos, "On the similarity between aortic and carotid pressure diastolic decay: a mathematical modelling study," *Sci. Rep.*, vol. 13, no. 1, pp. 1–9, 2023, doi: 10.1038/s41598-023-37622-y.

[39] G. F. Mitchell *et al.*, "Arterial stiffness, pressure and flow pulsatility and brain structure and function: The Age, Gene/Environment Susceptibility-Reykjavik Study," *Brain*, vol. 134, no. 11, pp. 3398–3407, 2011, doi: 10.1093/brain/awr253.

[40] W.-T. Wang, W.-L. Chang, and H.-M. Cheng, "The Relationship of Vascular Aging to Reduced Cognitive Function: Pulsatile and Steady State Arterial Hemodynamics," *Pulse*, vol. 10, no. 1–4, pp. 19–25, 2022, doi: 10.1159/000528147.

[41] S. Parittotokkaporn, D. De Castro, A. Lowe, and R. Pylypchuk, "Carotid Pulse Wave Analysis: Future Direction of Hemodynamic and Cardiovascular Risk Assessment," *JMA J.*, vol. 4, no. 2, pp. 119–128, 2021, doi: 10.31662/jmaj.2020-0108.

[42] I. B. Wilkinson *et al.*, "Heart rate dependency of pulse pressure amplification and arterial stiffness," *Am. J. Hypertens.*, vol. 15, no. 1, pp. 24–30, 2002, doi: 10.1016/S0895-7061(01)02252-X.

[43] J. K. Berkow and A. M. Brumfield, "System and Method for Characterizing Circulatory Blood Flow," US 9,002,440 B2, 2015.

[44] M. Cecconi, L. Evans, M. Levy, and A. Rhodes, "Sepsis and septic shock," *Lancet*, vol. 392, no. 10141, pp. 75–87, 2018, doi: 10.1016/S0140-6736(18)30696-2.

[45] A. L. Pauca, N. D. Kon, and M. F. O'Rourke, "Benefit of glyceryl trinitrate on arterial stiffness is directly due to effects on peripheral arteries," *Heart*, vol. 91, no. 11, pp. 1428–1432, 2005, doi: 10.1136/hrt.2004.057356.

[46] E. C. Schroeder, W. K. Lefferts, T. I. M. Hilgenkamp, and B. Fernhall, "Acute systemic inflammation reduces both carotid and aortic wave reflection in healthy adults," *Physiol. Rep.*, vol. 7, no. 15, 2019, doi: 10.14814/phy2.14203.

[47] B. Bollen Pinto *et al.*, "Metabolites Concentration in Plasma and Heart Tissue in Relation to High Sensitive Cardiac Troponin T Level in Septic Shock Pigs," *Metabolites*, vol. 12, no. 4, pp. 319–332, 2022, doi: 10.3390/metabo12040319.

[48] H. Ooi, W. Chung, and A. Biolo, "Arterial Stiffness and Vascular Load in Heart Failure," *Congest. Hear. Fail.*, vol. 14, no. 1, pp. 31–36, 2008.

[49] B. R. Clapp *et al.*, "Inflammation-induced endothelial dysfunction involves reduced nitric oxide bioavailability and increased oxidant stress," *Cardiovasc. Res.*, vol. 64, no. 1, pp. 172–178, 2004, doi: 10.1016/j.cardiores.2004.06.020.

[50] R. M. Bruno, L. Ghiadoni, G. Seravalle, R. Dell'Oro, S. Taddei, and G. Grassi, "Sympathetic regulation of vascular function in health and disease," *Front. Physiol.*, vol. 3, no. 284, pp. 1–15, 2012, doi: 10.3389/fphys.2012.00284.

[51] M. Carrara, A. Herpain, G. Baselli, and M. Ferrario, "A mathematical model of dP/dt max for the evaluation of the dynamic control of heart contractility in septic shock," *IEEE Trans. Biomed. Eng.*, pp. 1–1, 2019, doi: 10.1109/tbme.2019.2894333.

[52] J. E. Sharman, J. E. Davies, C. Jenkins, and T. H. Marwick, "Augmentation Index, Left Ventricular Contractility, and Wave Reflection," *Hypertension*, vol. 54, no. 5, pp. 1099–1105, 2009, doi: 10.1161/HYPERTENSIONAHA.109.133066.

[53] M. I. Monge García *et al.*, "Noradrenaline modifies arterial reflection phenomena and left ventricular efficiency in septic shock patients: A prospective observational study," *J. Crit. Care*, vol. 47, pp. 280–286, 2018, doi: 10.1016/j.jcrc.2018.07.027.

[54] Q. Pan *et al.*, "Pulsatility damping in the microcirculation: Basic pattern and modulating factors," *Microvasc. Res.*, vol. 139, no. July 2021, p. 104259, 2022, doi: 10.1016/j.mvr.2021.104259.

[55] F. Garcia-Polite *et al.*, "Pulsatility and high shear stress deteriorate barrier phenotype in brain microvascular endothelium," *J. Cereb. Blood Flow Metab.*, vol. 37,

no. 7, pp. 2614–2625, 2017, doi: 10.1177/0271678X16672482.

[56] H. Sun *et al.*, "Wave reflection quantification analysis and personalized flow wave estimation based on the central aortic pressure waveform," *Front Physiol.*, vol. 14, no. Feb 2023, p. 1097879, 2023, doi: 10.3389/fphys.2023.1097879.

[57] R. Manoj *et al.*, "Arterial pressure pulse wave separation analysis using a multi-Gaussian decomposition model," *Physiol Meas.*, vol. 43, no. 5, 2022, doi: 10.1088/1361-6579/ac6e56.